frontiers in Materials

ORIGINAL RESEARCH
published: 02 March 2022
doi: 10.3389/fmats.2022.826076

Hygrothermal Aging History of Amine-Epoxy Resins: Effects on Thermo-Mechanical Properties

Dennis Gibhardt, Christina Buggisch, Devin Meyer and Bodo Fiedler*

Institute of Polymers and Composites, Hamburg University of Technology, Hamburg, Germany

Epoxy systems are widely used as matrix resins for fiber reinforced polymers (FRP) and, therefore, often have to withstand harsh environmental conditions. Especially in marine and offshore environments, moisture or direct water contact leads to water absorption into the epoxy resin. As a result, the mechanical properties change during application. Since diffusion at room or colder temperatures is slow, industry and academia typically use accelerated aging methods at elevated temperatures for durability prediction. However, as the water-polymer interaction is a complex combination of plasticization, physical aging, and molecular interaction, all of these mechanisms are expected to be affected by the ambient temperature. To reveal the impact of aging time and temperature on the thermo-mechanical properties of an amine-epoxy system, this publication includes various hygrothermal aging conditions, like water bath and relative humidity aging at temperatures ranging from 8°C to 70°C and relative humidity from 20% to 90%. Thus, it is demonstrated *via* long-term aging, DMTA and FTIR investigations that, e.g., strength, stiffness, strain to failure, and the glass transition temperature (T_g) can differ significantly depending on aging time and temperature. For example, it can be shown that water absorption at cold temperatures leads to the strongest and longest-lasting reduction in strength, although the maximum water absorption amount is lower than at higher temperatures. For the application, this means that strength differences of up to 26% can be obtained, depending on the aging method selected. Furthermore, it can be shown that conventional prediction models, such as Eyring correlation, which consider the mobility of the molecular structure for the prediction of thermo-mechanical properties, can only be used to a limited extent for prediction in hygrothermal aging. The reasons for this are seen to be, in particular, the different characteristics of the water-polymer interactions depending on the aging temperature. While plasticization dominates in cold conditions, relaxation and strong water-molecule bonds predominate in warm conditions.

Keywords: water, plasticization, physical aging, strength, temperature, durability, FTIR

OPEN ACCESS

Edited by:
Patricia Maria Frontini, CONICET Mar del Plata, Argentina

Reviewed by:
Veronique Michaud, Ecole Polytechnique Fédérale de Lausanne, Switzerland
Sébastien Touzain, Université de la Rochelle, France

****Correspondence:***
Dennis Gibhardt
dennis.gibhardt@tuhh.de

Specialty section:
This article was submitted to Polymeric and Composite Materials, a section of the journal Frontiers in Materials

Received: *30 November 2021*
Accepted: *24 January 2022*
Published: *02 March 2022*

Citation:
Gibhardt D, Buggisch C, Meyer D and Fiedler B (2022) Hygrothermal Aging History of Amine-Epoxy Resins: Effects on Thermo-Mechanical Properties. Front. Mater. 9:826076. doi: 10.3389/fmats.2022.826076

1 INTRODUCTION

To achieve efficient and sustainable use of raw materials and energy, structures made of lightweight composites and thermosetting polymers or adhesives are in wide use today (Gagani et al., 2019; Budhe et al., 2018; Rocha et al., 2017), while the demand is still increasing (Amano, 2017); but to make a decisive contribution to the energy and mobility transition, their lightweight and durability potential has to be exploited even further. It is especially mandatory to extend the operating life of structures and components even under harsh environmental conditions while at the same time ensuring safe operation. Therefore, deep knowledge about how composites and their polymer matrices change their properties during application over time and under the influence of water, moisture, and different temperatures is required. Numerous studies have already dealt with the durability in case of water absorption (Gagani et al., 2019; Humeau et al., 2018) or various operating temperatures in the past (Kraus and Trappe, 2021; Tcharkhtchi et al., 2015). Most of them have in common that, due to slow diffusion rates at moderate ambient temperatures, they rely on accelerated aging processes at elevated temperatures for prediction of property development (Ilioni et al., 2019; Bordes et al., 2009; Jaksic et al., 2018). Thanks to these studies, it is known that absorbed water can cause significant changes in thermo-mechanical properties due to simultaneously occurring plasticization and relaxation (physical aging) (Le Guen-Geffroy et al., 2019; Zheng et al., 2004). Since the plasticizing effect of water is understood as a reduction of the intramolecular forces by increasing the chain distances, it is often compared with an increase in ambient temperature. Consequently, models for predicting mechanical properties of dry polymers in relation to their glass transition temperatures (T_gs) and the ambient temperature like modifications of the Eyring (Banea et al., 2011; Chai, 2004) or Kambour (Kambour, 1983) correlations were also applied for wet polymers (Ilioni et al., 2019; Le Gac et al., 2017). Generally, it has been shown that the tensile strength and the T_g are the most affected properties by water absorption as they can be reduced by a factor of 2 or even more (Zhou and Lucas, 1999b; Startsev et al., 2018).

The equilibrium amount of water absorbed in polymers or, respectively, epoxies in the specific case mainly depends on the polymer's structure (Bellenger et al., 1989; Colin, 2018). Historically, a distinction was often made between "volumetrically" determined and "interactionally" determined explanations. Here, the volumetric approaches mainly consider the absorption into the free volume, which might be varied by the curing degree and temperature, and into the space, which is a consequence of undesirable defects such as micro-pores or cracks (Enns and Gillham, 1983). Following this approach, interactions between water and the polar sites of the polymer network are neglected for the most part. In contrast, it is just these water-polymer network interactions that are nowadays often considered to dominate water uptake (Musto et al., 2002; Colin, 2018). Therefore, it was shown that water molecules are attracted by the polarity of the polymers chemical structure and that water also binds with these molecule segments by hydrogen bonds (Zhou and Lucas, 1999a; Gaudichet-Maurin et al., 2008). Furthermore, spectroscopy and absorption-desorption experiments showed that at least three conditions in which the water interacts with the molecular network can be identified. They are defined as free or unbound water, weakly bound water (type I) which forms one hydrogen bond with the network, and strongly bound water forming two hydrogen bonds (type II) (Zhou and Lucas, 1999a). While it was postulated by Zhou and Lucas (1999b) that the type II water bonding increases the wet epoxy's T_g, effects on other mechanical properties like strength, stiffness, and failure strain were not reported. Besides gravimetric measurements, FTIR spectroscopy is known to be used for determination of the water content (Krauklis A. E. et al., 2018; Muroga et al., 2017) and type of water–network interaction (Cotugno et al., 2001; Musto et al., 2000) in polymers. Both measurement methodologies are used within this study to compare the water absorption in dependence of the aging environment.

More recently, Le Guen-Geffroy et al. (2019) published an extensive investigation on the coupling of plasticization and physical aging for an amine-epoxy. In order to separate the effects of both phenomena, an artificial state mostly free of relaxation achieved by thermal rejuvenation was used as a basis. Aging in air and water allowed them to draw valuable conclusions, showing that physical aging is dramatically accelerated due to the presence of water, which reduces the T_g significantly and thus the distance between aging temperature and T_g. Furthermore, it was shown that physical aging, on the contrary, has minimal effect on plasticization. Even though both processes were shown to be reversible during high temperature-treatment, this is not feasible in most applications. The temperature range was enlarged within the present study to cold temperatures below room temperature and warm temperatures above T_g, not to focus only on accelerated aging conditions, as it is regularly done (Krauklis A. et al., 2018; Rocha et al., 2017). Thus, the aging was conducted in environments from 8°C to 70°C. Furthermore, aiming to enlarge the properties under consideration, tensile and DMTA tests as well as FTIR spectroscopy were performed for various time-temperature combinations. Thus, the thermo-mechanical behavior of an amine-epoxy is studied and related to its properties after manufacturing. After the epoxy is first thoroughly characterized, water absorption and the resulting thermo-mechanical properties are examined in more detail. Afterwards, it is shown that with the help of DMTA, fundamental differences between individual conditions can be revealed, although the water content and strength can be identical.

2 MATERIALS AND METHODS

2.1 Materials

The epoxy resin system under investigation is the resin Hexion EPIKOTE™ Resin MGS™ RIMR 135 and the amine hardener EPIKURE™ Curing Agent MGS™ RIMH 137, which is a low-viscosity and slow-hardening system applicable for infusion and

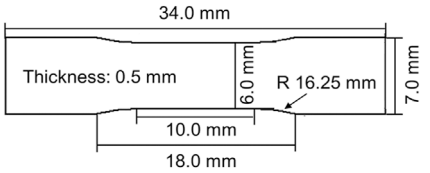

FIGURE 1 | Specimen geometry for tensile and DMTA tests with given dimensions.

resin transfer molding (RTM) processes. The resin component consists of bisphenol A diglycidyl ether (DGEBA) (75%–90%) and 1,6-hexanediol diglycidyl ether (HDDGE) (10%–20%). Polyoxypropylenediamine (POPA) (50%–75%) and isophorone diamine (IPDA) (25%–50%) are the reactive amines used in the hardener. The epoxy system is commercially widely used in wind energy and maritime applications.

2.2 Sample Manufacturing and Preparation

A closed mold RTM process with a 0.5 mm thick aluminum frame was used for epoxy plate manufacturing. The resin was mixed with a ratio of 100:30 parts resin and hardener (by weight) and degassed using a vacuum stirrer prior to infusion. Afterwards, the resin was infused under vacuum and held at 50°C for 15 h. After demolding, an additional post-curing process at 80°C for 16 h was implemented according to the manufacturers' recommendation. All specimens for this study were milled using a 1.8 mm diamond milling cutter. A dogbone-shaped specimen geometry in reference to the DIN EN ISO 527-2 1BA standard as shown in **Figure 1** has been defined and used. Before testing or aging, the edges of all specimens were polished with 2500 grit size sandpaper in a defined process of 20 repetitions per side. To ensure uniform dryness, all specimens were dried in a vacuum oven at 40°C for at least 72 h prior to testing or hygrothermal aging, respectively.

2.3 Hygrothermal Aging and Water Absorption

The hygrothermal aging conditions in this study include aging in both water bath and humid air over a temperature range between 8°C and 70°C and relative humidities between 20% and 90%. For conditioning in humid air, a Memmert ICH110 climate chamber was used. All specimen were weighed before and after aging, while three of each condition were weighed also regularly during aging. For weight measurements, a Metler Toledo AT261 scale with a precision of 0.01 mg was used. All specimens were carefully wiped dry before weight measurements. The relative weight change M_t was calculated by the following definition:

$$M_t = \frac{(m_t - m_0)}{m_0} \cdot 100, \quad (1)$$

where m_0 is the dry reference weight after initial drying and m_t is the weight of the aged sample at time t. Care was taken to ensure that all samples were tested within 30 min of removal from conditioning, as drying at ambient conditions can otherwise affect the results. A detailed overview of all conditions and aging durations is given in **Table 1**. For most configurations, the tests were performed as soon as saturation was reached. In addition, tests after various aging duration were performed for some specific conditions to investigate the effect of aging time. In the case of conditioning in 40°C water, additional tests with re-dried and rejuvenated specimen were performed. Re-drying was done in a vacuum oven at 40°C for 169 h until no further weight change was measured within 24 h. Since the weights after re-drying were not lower than the initial dried weight, it can be confirmed that there is no material loss during water aging. The rejuvenation process was done according to Le Guen-Geffroy et al. (2019), where the specimens were first sealed in plastic bags, heated up to 90°C for 5 min in a water bath, and afterwards quenched in 10°C cold water. The rejuvenation process for dry specimens was done at boiling water conditions to assure a temperature above the dry T_g.

2.4 Tensile Testing and Dynamic Mechanical Thermal Analysis

For tensile tests and DMTA, a Netsch Gabo Eplexor 500 equipped with a 500 N load cell was used. Tensile tests were performed for dry reference and aged specimens with a speed of 1 mm/min until failure. Dry reference specimens were also tested under various ambient temperatures ranging from −20°C to 60°C. During temperature testing, each sample was held at the specific temperature for 5 min before starting the test to assure a homogeneous sample temperature. Ultimate tensile strength σ_t, Young's modulus E and strain to failure ϵ were evaluated for all tensile test specimens. Stress–strain curves were additionally analyzed to compare the non-elastic behavior. The number of tested tensile samples per single condition was regularly $n = 3$ as the standard deviation was small. DMTA measurements were run from 20°C to 120°C with a frequency of 1 Hz and heating rate of 3°K/min. T_g was calculated as $T_{g,onset}$ of the storage modulus E′. Therefore, the intersection between linear regressions through the low-temperature results and the transition-zone are taken for

TABLE 1 | Hygrothermal aging conditions and durations of specimen for mechanical testing. A distinction is made between aging in a water bath (WB) and in a climatic chamber at relative humidity (RH).

Type	Temperature in °C	Rel. Humidity in %	Aging duration in h
WB	8	100	24, 72, 171, 1028, 2600
WB	22	100	400, 2600
WB	30	100	1000
WB	40	100	400, 2600
WB	50	100	76, 189, 2600
WB	70	100	400
RH	10	90	950
RH	22	20, 50, 80, 90	250, 650
RH	30	70	300
RH	36	50	336
RH	40	80	215
RH	50	50, 80	500, 325

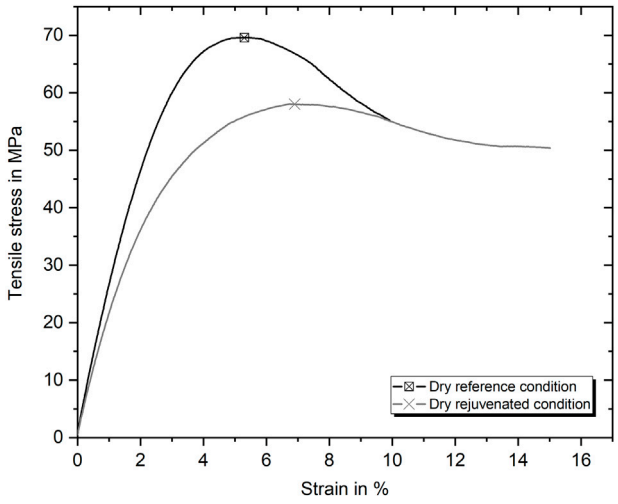

FIGURE 2 | Representative stress–strain curves of dry reference and dry rejuvenated condition.

determination of T_g as it is typically done in accordance with ISO 6721.

2.5 FTIR Measurements

NIR Fourier transform infrared spectroscopy (FTIR) was used to analyze the polymer-water interaction further. Various spectra were recorded in transmission mode from 1,500 cm^{-1}–7,500 cm^{-1} using a Bruker Tensor 2 FTIR spectrometer with a resolution of 2 cm^{-1}. Each acquisition spectrum is composed of eight single measurements, and for each conditioning state, at least nine measurements were conducted on three specimens. For further analysis, the spectra were first checked for irregularities, baseline shifted, and normalized. The peak at a wavenumber of about 5,250 cm^{-1} is considered to evaluate the water content inside the epoxy. Therefore, the area of the peak (peak integral) is determined using Origin 2019 software.

3 EXPERIMENTAL RESULTS AND DISCUSSION

3.1 Characterization of the Epoxy in Dry Condition

Since the properties of epoxies are relatively dependent on the chemical composition, the particular manufacturing process, the degree of cure, and the time–temperature history, the system under study is first characterized in initial conditions. In detail, the tensile stress–strain behavior (**Figure 2**), DMTA response in terms of E′ and tan(δ) versus temperature curves (**Figure 3**), and FTIR analysis (**Figure 4**) will be presented. Because hygrothermal aging involves simultaneous plasticization and physical aging, the condition of the material after the manufacturing process is also checked essentially. For this purpose, the initial (briefly dried) material as it is used also in composite manufacturing is compared with the artificial state mostly free of any relaxation and physical aging as produced by the rejuvenation process. However, as the epoxy will not be in this artificial state while used in applications, the investigation focuses mainly on the development of the properties based on the material condition after regular manufacturing.

The stress–strain curves in **Figure 2** highlight the differences of the tensile behavior in dependence of the physical aging extent, which is reached either by manufacturing or by an ideal, mostly relaxation free state. It can be seen that the yield strength and stiffness are significantly increased in the dry reference condition, while the strain at break is reduced. In numbers, the strength increases by about 12.1 MPa (18.5%), the Young's modulus by about 0.375 GPa (15.6%), and the strain to failure decreases by about 5.5%. Basically, the epoxy shows a typical elastoplastic

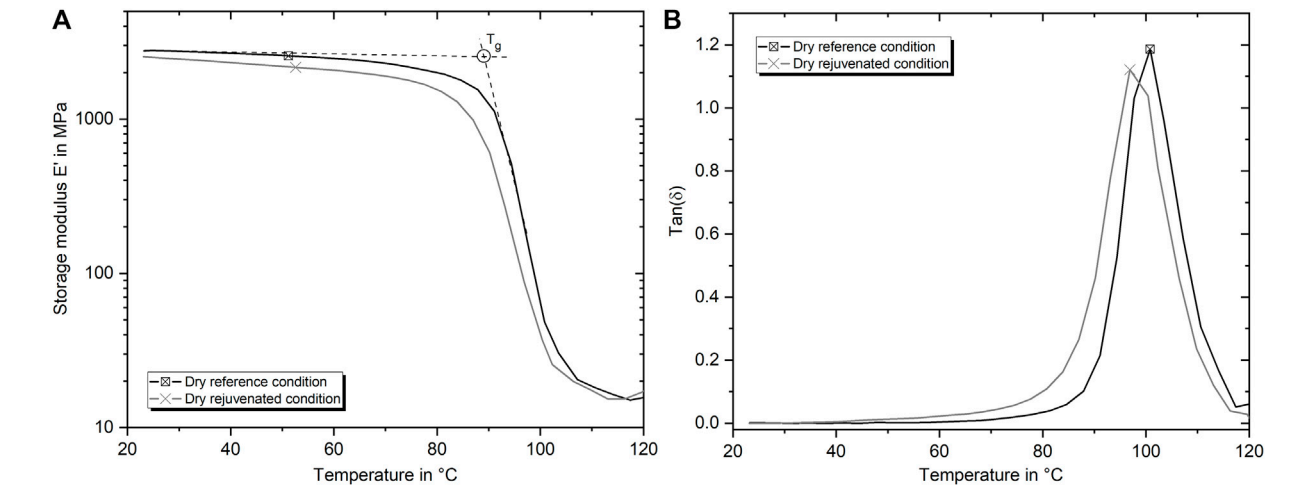

FIGURE 3 | Representative DMTA curves of E′ **(A)** and tan(δ) **(B)** versus temperature for dry reference and dry rejuvenated condition.

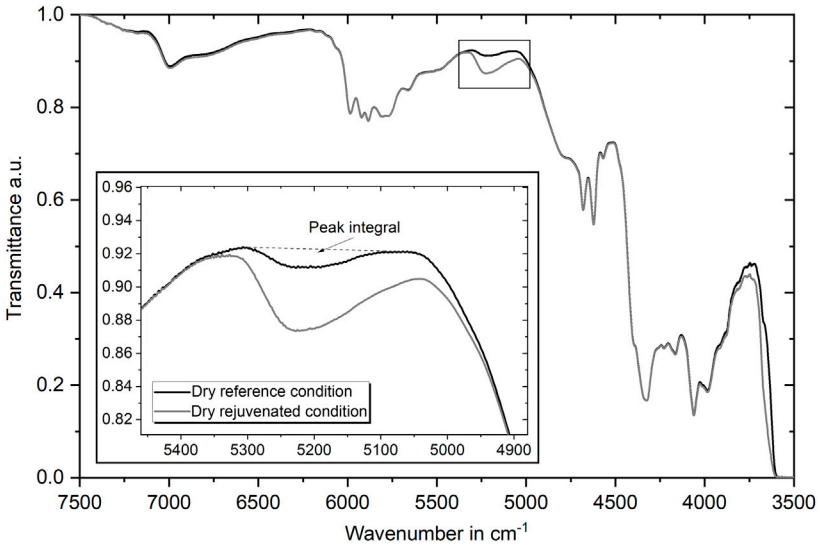

FIGURE 4 | Representative normalized transmittance FTIR curves in the NIR range for dry reference and dry rejuvenated condition. Enlarged illustration of the OH-peak at 5,250 cm^{-1} as a representation of the water content.

behavior with first a linear elastic part for low strains and a pronounced plastic yield part for higher strains in both conditions. The ability of the amine-epoxy investigated to undergo large plastic deformation also in dry conditions was recently shown to be based on load-dependent intramolecular and intermolecular interactions (Doblies et al., 2021). The mechanical properties of the dry reference condition (strength: 69.9 MPa, modulus: 2.75 GPa and failure strain: 10%) are used as benchmark properties within this study.

To get an overview to which extent the physical aging due to the manufacturing process in the reference condition affects the thermo-mechanical properties, DMTA results are presented in **Figure 3**. Again, the results confirm the difference in stiffness, which was also evaluated for the tensile tests. Furthermore, it gets evident that the T_g of the rejuvenated specimens is with 86.5°C about 2.9°C lower than the T_g of the reference specimens, which is 89.4°C. In addition to the difference in T_g, which can be identified by the shift of the peak to lower temperatures, the tan(δ) curves also reveal that material damping in the rejuvenated condition begins at much lower temperatures. The peak has not only shifted but also become wider at the base.

Finally, **Figure 4** shows the FTIR curves obtained in transmission for the NIR range from 3,500 cm^{-1} to 7,500 cm^{-1}. As both curves overlap for almost the entire range, it can be noted that differences in the physical aging condition cannot be easily identified using this specific setup. The only significant difference of the spectra can be seen in the peak around the wavenumber of 5,250 cm^{-1}, which is associated with the bending and stretching modes of the water molecule's OH group (Krauklis A. E. et al., 2018). As the peak area is increased for the rejuvenated specimens, it can be assumed that they have absorbed some minor amount of water during the process. Taking the peak area and, therefore, the low amount of absorbed water into account, it is expected that this will decrease the strength only to a small extent of some MPa. The peak area in terms of the presented integral is taken to monitor the water content of various dry and wet conditions during this investigation as proposed by Krauklis A. E. et al. (2018). Thus, the peak integral of the dry reference conditions is 1.33, while it is 5.70 for the rejuvenated case. After aging for 400 h in 40°C water, the value is largely increased to 34.60 for comparison. In conclusion, it can be stated that the reference specimens contain only a marginal amount of water, which the initial drying process could not remove.

3.2 Water and Moisture Absorption

Because the mechanical properties of epoxy basically change with the diffusion of water into the molecular structure, the water absorption characteristics are presented first. The equilibrium water uptake of the amine-epoxy resin under investigation is with about 3.0 m% at 50°C immersed water bath conditions within a typical range. Values reported for similar systems cover a range from 1.0 to 5.0 m% (Colin, 2018; Capiel et al., 2018; Humeau et al., 2018; Abdelkader and White, 2005). In more detail, as shown exemplarily in **Figure 5**, the water uptake behavior of the epoxy specimen depends both on the ambient temperature and on the relative humidity and thus on the activity of the water. The weight change curves for up to 120 days (symbols experimental data, lines Fickian absorption model) reveal that the maximum water uptake increases with temperature from 8°C to 50°C by 0.4 m% which is a significant rise of about 15%. Although this is, to some extent, in contrast to the results of Zhou and Lucas (1999a), stating that equilibrium water uptake of epoxies is independent of the aging temperature, it is essential to note the corresponding temperature range. While Zhou and Lucas (1999a) investigated aging temperatures ≥45°C, which already provide much external energy for the water absorption, the cold water absorption presented in this study provides by far less

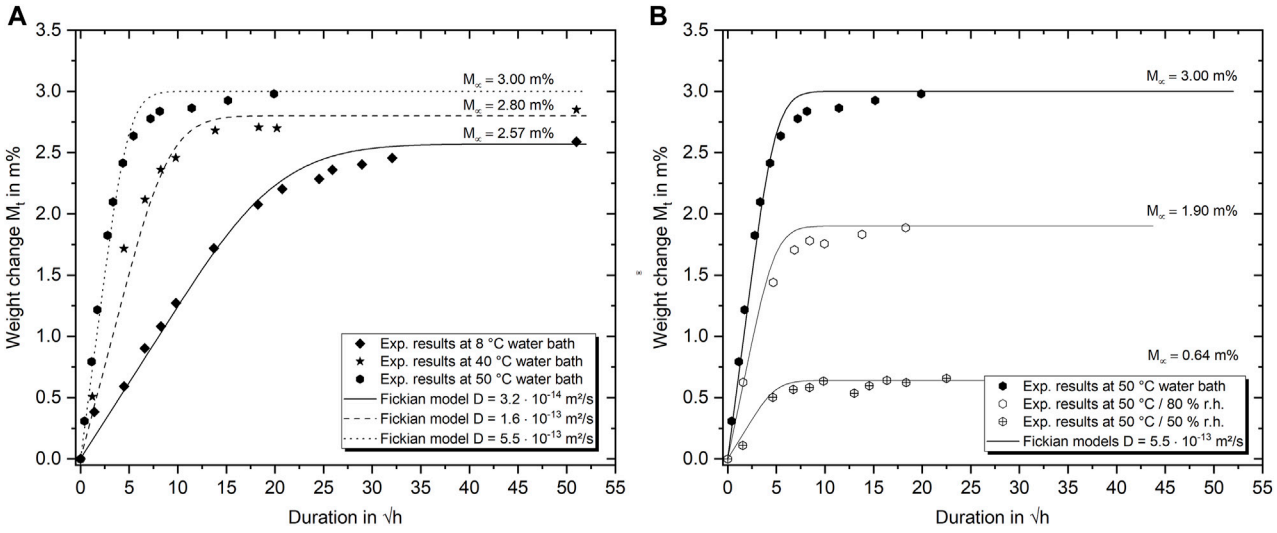

FIGURE 5 | Exemplary weight gain curves for epoxy aging in water of different temperatures **(A)** and humid air at 50°C and different relative humidity **(B)**. Symbols represent experimental gravimetric measurements, lines indicate Fickian absorption models.

external energy. More recent studies on the water absorption behavior of physically aged and un-aged epoxy coatings by Elkebir et al. (2020) also covered a wide temperature range from 30°C to 60°C. Similarly as in the present case, the authors found temperature-dependent differences for the maximum water absorption. Furthermore, they were able to show that physical aging has a severe impact on the water absorption content (Elkebir et al., 2020). In detail, it was revealed that the water absorption could be depressed by more than 1.0 m% due to physical aging. Similarly, at low temperatures, both water activity and the mobility of the molecular network are significantly reduced. Since the epoxy's polarity and chemical structure are independent of the ambient temperature and the free volume below T_g is only weakly temperature dependent in the range considered, it is unlikely that these are the reasons for the different maximal water absorption. Therefore, the proposed explanation for this behavior could be that there is not enough energy available in the system at low temperatures to allow the water molecules to diffuse into all the theoretically available regions of the free volume (Ding et al., 2001; Elkebir et al., 2020). For example, due to reduced molecular motion and steric hindrance, not all water molecules could reach the vicinity of the particularly polar chain parts like hydroxyl groups. As the ambient temperature increases, more and more of these attractive but inaccessible regions can be entered by the diffusing water. For the specific DGEBA/HDDGE/POPA/IPDA system under investigation, the temperature at which no further maximal weight gain can be identified is about 50°C. Increasing the temperature to 70°C does consequently not result in any further water absorption compared with aging at 50°C. This is furthermore remarkable, as the results also highlight that the maximum water absorption is not increasing at aging temperatures higher than the current wet T_g, which is about 65°C at saturation (measured directly after extraction from the water bath with DMTA as described in **Section 2.4**). Therefore, the more pronounced increase in the free volume above T_g has no significant impact on the equilibrium water content.

As expected, increasing relative humidity increases the maximum water absorption in humid air (**Figure 5B**) significantly. This phenomenon enables homogeneous water distributions within individual specimens at various equilibrium water contents and with similar temperature histories. The diffusivity in terms of the diffusion coefficient D is known to be exceedingly temperature-dependent but independent of the relative humidity. This is also confirmed by the Fickian water absorption models for thin sheets presented in **Figure 5**. While the simple Fickian absorption models can describe the absorption process up to about 80% of the maximum weight change quite satisfying, clear deviations can be found in the transition from the linear to the asymptotic range. Even if these deviations are a known phenomenon and can be better described by more complex diffusion theories (LaPlante et al., 2008), they are not included in this publication. More decisive is the observation that water absorption does not lead to weight gain or loss once saturation is reached for the entire temperature range studied, which is also consistent with the studies of Krauklis A. et al. (2018). Taking the temperature dependent diffusion coefficients presented in **Figure 5** into account, it is possible to calculate the activation energy of the water absorption by the following Arrhenius relationship:

$$D_T = D_0 \exp^{\frac{-Q}{T \cdot R}} \quad (2)$$

with the diffusion coefficient D_T at temperature T, the temperature independent diffusion coefficient D_0, the molar gas constant R and the activation energy Q. Evaluating the results for water diffusion at different temperatures the activation energy Q was found to be 47.2 kJ/mol, which is well

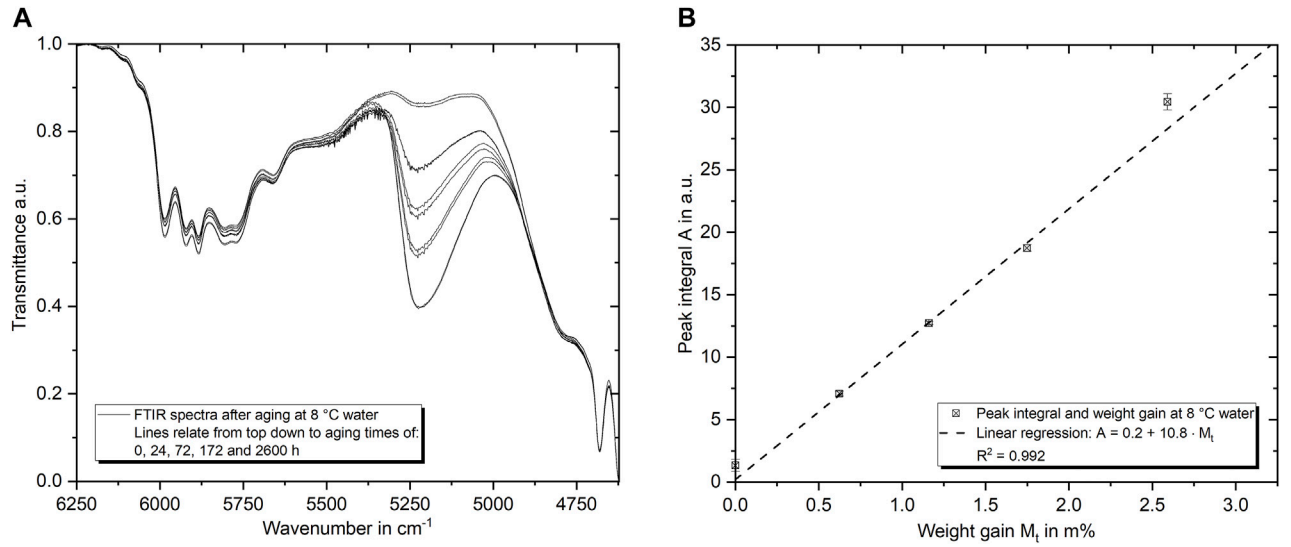

FIGURE 6 | FTIR spectra of the epoxy aged in 8°C water in the region of the water absorbance band (5,250 cm^{-1}) for several aging times **(A)**. In **(B)** the correlation between the peak integral and the weight gain (gravimetric measure) is shown. A linear regression indicates a high level of determination.

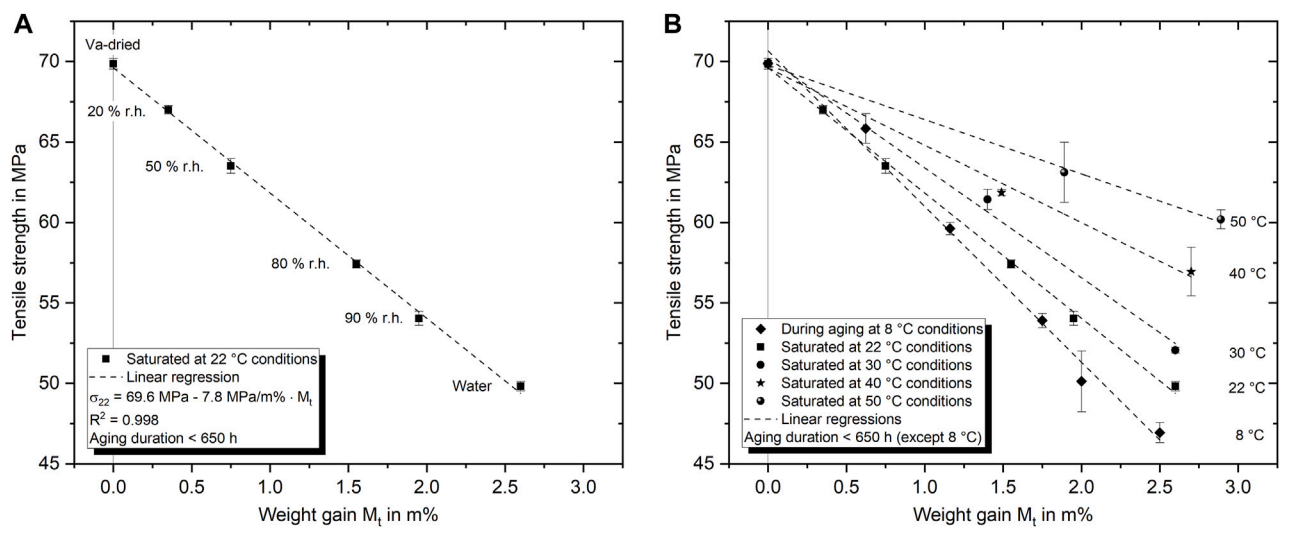

FIGURE 7 | Relation between maximum tensile yield strength and amount of absorbed water at 22°C **(A)** and absorbed water at various aging temperatures **(B)**. All specimens were aged until homogeneous saturation conditions were achieved.

in line with the results presented e.g. by Zhou and Lucas (1999a) who calculated activation energies between 43.5 kJ/mol and 51.1 kJ/mol.

In addition to gravimetric measurements, FTIR spectroscopy is used to determine the water content within the epoxy. This is exemplarily shown in **Figure 6A** for the water absorption in 8°C water for a duration of up to 2,600 h. As introduced before, it is evident that the peak at about 5,250 cm^{-1} raises during water absorption. In **Figure 6B**, the weight gain and the peak integral are compared. The linear regression, displayed with the dashed line, indicates high accordance of both techniques. Therefore, the maximum water content can also be evaluated using spectroscopy data and accordingly confirms the peak integral evaluation for the long term aging under various temperatures differences in maximum water content found by weight measurements. The average peak integral of 8°C aging after 2,600 h is 13.3% smaller than the 50°C integrals. Considering the regression presented in **Figure 6B**, this corresponds to a weight gain difference of about 0.43 m%, which is exactly the difference measured gravimetrically.

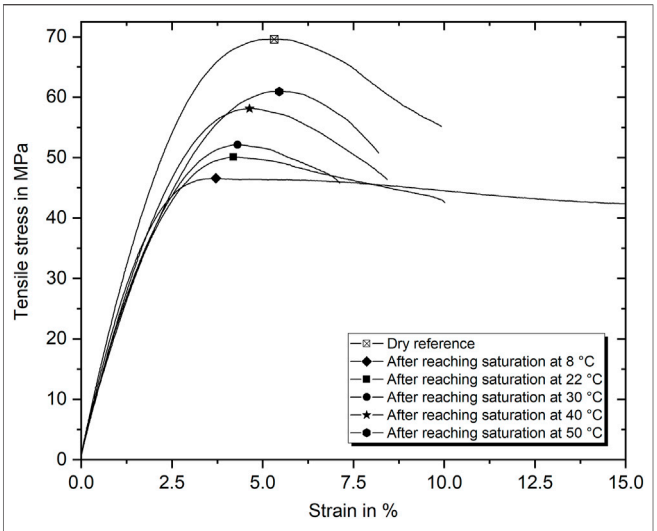

FIGURE 8 | Representative stress–strain diagrams of specimen aged at various temperatures. Tests were performed as soon as saturation was reached.

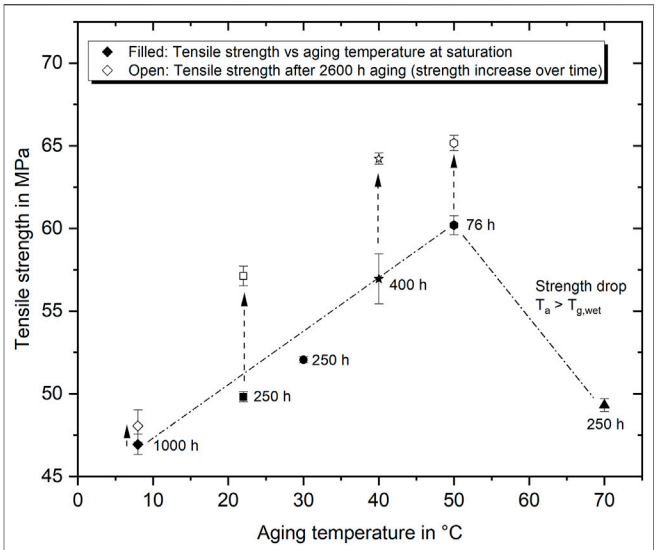

FIGURE 9 | Correlation between water bath aging temperature and maximum tensile yield strength shortly after reaching saturation (filled symbols) and after 2,600 h of aging (open symbols).

3.3 Impact of Aging Temperature on Tensile Properties

In **Figure 7A** the maximum tensile yield strength is plotted in relation to the equilibrium content of absorbed water at 22°C for various relative humidities and a water bath immersion. In all cases, the corresponding tensile tests were executed within 650 h (1 month) of aging, which is shortly after saturation has been reached. The maximum drop in tensile yield strength under these conditions is 20.1 MPa (28.8%) from vacuum dried reference strength (69.9 MPa) to water immersed condition (49.8 MPa). The results show that the strength appears to be linearly dependent on the amount of absorbed water. So, a linear regression describing this correlation can be formulated as

$$\sigma_{22} = 69.8\,\mathrm{MPa} - 7.8\,\mathrm{MPa/m\%} \cdot M_{\infty}(\phi), \tag{3}$$

where σ_{22} is the tensile yield strength after aging at 22°C and $M_{\infty}(\phi)$ is the weight gain at saturation as a function of the relative humidity ϕ. So far, the results suggesting a clear correlation between absorbed water content and tensile strength are in line with what has been shown previously by authors such as Ilioni et al. (2019). In contrast, additional investigations on specimens aged at various other temperatures but still tested under homogeneous saturation conditions (within about 1 week after saturation was reached) disclose that the tensile strength of the epoxy is not a simple function of the amount of absorbed water. Rather, it becomes evident that the ambient temperature at which the water was absorbed has a decisive influence on the tensile strength. Knowing the amount of absorbed water exclusively without information about the temperature history is not enough to predict the tensile strength. Nevertheless, the strength seems to follow a linear relationship with the amount of absorbed water for each aging temperature. Contrary to what might be intuitively expected, the strength increases with increasing aging temperature. Moreover, this implies that the higher water absorption at elevated temperature already shown in **Section 3.1** has no additional negative influence on the tensile strength. Again, all results shown in **Figures 7**, **8** are acquired shortly after reaching saturation.

3.4 Stress–Strain Behavior of Epoxy Saturated at Different Temperatures

Representative stress–strain curves for wet saturated specimens after aging in water of different temperatures are presented in **Figure 8**. The stress–strain curve of the dry epoxy in the reference condition is shown for comparison as well. In addition to the fact that the strength decreases with decreasing aging temperature, it also appears that the maximum strain at break is increasing or decreasing depending on the type of conditioning. While water absorption at 8°C significantly enlarges the failure strain to more than 20%, at 50°C, a decrease is apparent. Furthermore, defined yield points and additional strain-softening with pronounced plastic deformation are apparent for all conditions. Basically, the stiffness is slightly lower in all saturated conditions than in the dry condition (from 2.5 GPa for 50°C to 2.7 GPa for 8°C aging). This leads to clear differences at strains of about 3%, which mark the beginning of the yielding region. The behavior after cold water aging is particularly striking since, in this case, with increased elongation, almost no stress loss occurs. Under these specific conditions, the plasticizing effect of the water absorption comes into full effect. Since the amount of water absorbed is similar for the considered conditions, the stress–strain behavior is significantly influenced by the hygrothermal history defining the water-epoxy molecule interaction.

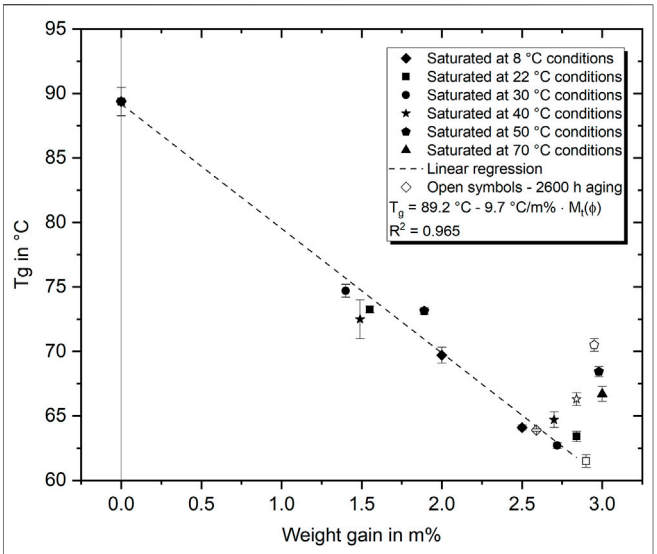

FIGURE 10 | Relation between water absorption content and T_g. A distinction is made between aging times: shortly after reaching saturation (filled symbols) and after 2,600 h of aging (open symbols).

3.5 Strength Development During Sub and Above T_g Aging

The tensile strength at saturation after aging in water of various temperatures and different aging times is presented in **Figure 9**. Also in this case, all tensile tests were performed at room temperature. Again, compared to the dry strength, it is evident that the wet strength decreases more, the colder the aging temperature is. This applies over a range from 8°C to 50°C. Furthermore, testing after long aging of at least 2,600 h (minimum 2 month after saturation was reached) reveals that the tensile strength increases significantly with an extension of the aging duration. The rate of strength increase is higher, the higher the surrounding temperatures are, which is in line with the Kohlrausch-Williams-Watts (KWW) correlation taking temperature-dependent relaxation time into account (Le Guen-Geffroy et al., 2019). Furthermore it can be seen that the strengths apparently converge to a maximum value of about 65 MPa at very long aging times. While this is already reached after about 2,600 h at 40 and 50°C, the underlying processes are much slower at colder temperatures.

In contrast, aging at 70°C also largely decreases the strength to about 49.3 MPa, which is a drop of 29.3% compared to the dry strength. This result corresponds well with the strength reported by Krauklis A. et al. (2018) for the same epoxy system aged at 60°C in water. The significant difference between aging in environments of up to 50°C and at higher temperatures can be explained by the fact, that the T_g is drastically depressed due to water absorption. In the specific case the water-saturated epoxy has an aging condition-dependent T_g of about 61.5°C –66.5°C (shown in **Figure 10**). The resulting T_gs are close but even lower than the hottest aging condition at 70°C. As the epoxy is not in a glassy state during the 70°C aging condition, it can be assumed that the water–epoxy interaction is also different. Following the reasoning proposed by Zhou and Lucas (1999a), or more recently Le Guen-Geffroy et al. (2019), there will be mainly two effects coming into play. The first is considering the type of bond state that the water can form with the epoxy network. In this context, Zhou and Lucas (1999a) showed that the fraction of type II bound water increases with increasing aging temperature and duration, at least for sub-T_g aging. The second effect is the assumption that physical aging will be eliminated entirely or depressed at temperatures above T_g, as the molecular network is more mobile and the free volume significantly enlarged (Le Guen-Geffroy et al., 2019). Therefore, especially a comparison of the cold water (8°C) and above-T_g aged samples allows drawing some conclusions on the proportions of these two mechanisms to the development of the tensile strength. As the degree of additional physical aging in short-time, low temperature aged epoxy is exceedingly small and probably negligible in above-T_g aged samples; differences of the strength might be related to the bond type of water and epoxy. In this regard, it is reasonable to assume that the proportion of type II bound water due to 8°C aging is very small, while it could be considerably higher for 70°C. The tensile strength difference of about 2.5 MPa (5.3%) is accordingly attributed to the higher proportion of water incorporated more strongly into the molecular structure (type II). Equally, this also means that most of the strength recovered over time during sub-T_g aging results from physical aging.

3.6 Impact of Hygrothermal Aging at Various Temperatures on T_g

The correlation of water absorption content and T_g is displayed in **Figure 10** for both aging in humid air and water until saturation. The plotted linear regression (considering temperatures up to 40°C), stating a T_g decrease of about 9.7 MPa/m%, fits well to the experimental results typically reported for amine-epoxies (Fernández-García and Chiang, 2002). This interrelation is usually described with the polymer-diluent model or the Simha-Boyer equation (Papanicolaou et al., 2006; Le Guen-Geffroy et al., 2019). However, significant deviations from this expected behavior are found particularly for aging at high temperatures and with longer aging time. Therefore, the development of the T_g over aging time is presented in **Figure 10** in terms of open symbols as well. For warm water aging at 40°C and 50°C, the results show a T_g increase of 1.6°C and 2.1°C respectively after 2,600 h compared to the short-term results reached directly after saturation. During aging under room temperature or in cold water, on the contrary, the T_g did not increase in the same period. Thus, it is evident that the T_g decreases significantly more due to the plasticizing effect of the water absorbed than it increases due to physical aging or an increase in the amount of type II bound water. Compared with the strength results presented in **Figure 9**, it becomes clear that the strength increase over time is mainly independent of the T_g development. Assuming that T_g is a measure of the mobility of the molecular structure, it follows that the reduction of free volume and the rearrangement of chain segments (physical aging) under the presence of water hardly leads to an impediment of mobility

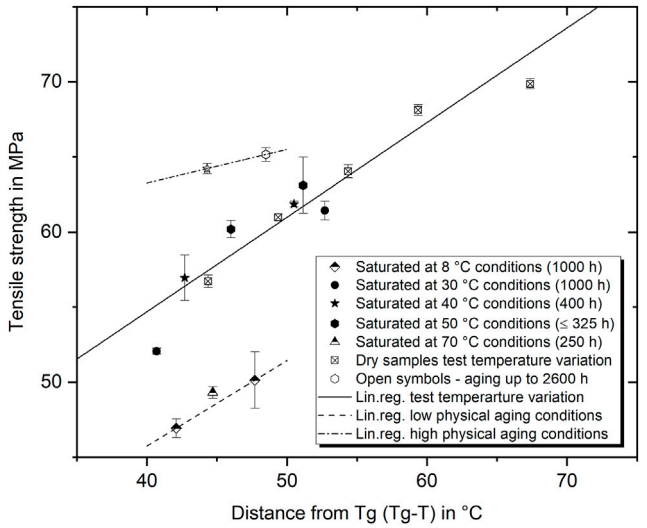

FIGURE 11 | Tensile strength in correlation to the distance between T_g and testing temperature T (T_g – T) for several water aged conditions and dry specimen at various temperatures.

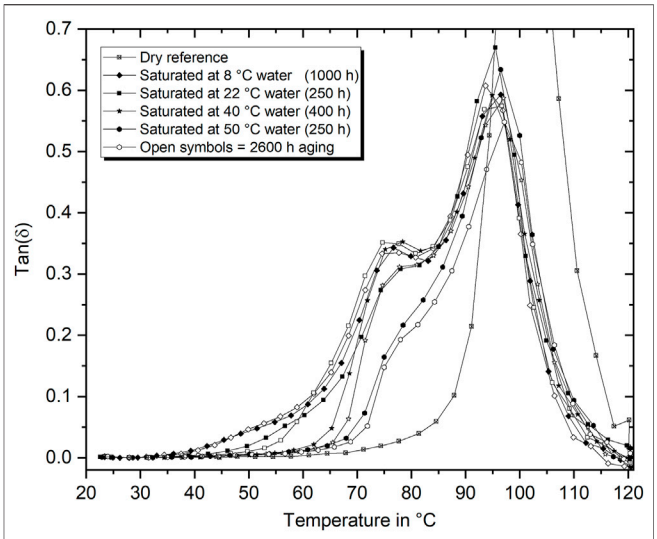

FIGURE 12 | Tan(δ) vs. temperature curves after aging in water baths between 8°C and 50°C for short-term saturated conditions (filled symbols) and long-term aging (2,600 h) (open symbols).

at room or colder temperatures. At higher temperatures, the change in T_g indicates a water-molecule interaction that reduces the mobility of chain segments. In summary, this is a strong indication that there is an increased formation of type II bound water with higher immersion temperatures and longer duration, similarly as proposed by Zhou and Lucas (1999b). Another important finding that can be derived from the presented results is that there seems to be a temperature threshold at which the polymer–water interaction changes more fundamentally. In detail, it can be identified that the wet T_g of the epoxy aged at temperatures ≥40°C is considerably higher than at lower temperatures even after long-term aging.

3.7 Tensile Strength Predictions Based on T_g Considerations

As the tensile strength of polymers is a consequence of their physical and chemical condition, this information can be used for property predictions. In the past, it was shown that the strength is especially affected by the mobility of molecular chains and segments, which the T_g of the polymer usually reflects (Tcharkhtchi et al., 1999). In detail, many authors found semi-empirical relations between the strength of a polymer and the difference between the T_g and the ambient testing temperature (Kraus and Trappe, 2021). For most polymers and epoxies as well, the tensile strength decreases linearly with increasing testing temperatures. The underlying relationship is represented by the Eyring equation, which is frequently used in the following form:

$$\sigma_y = A \cdot \left(T_g - T\right) + B, \tag{4}$$

where σ_y is the tensile yield strength, T is the testing temperature, and A and B are individual constants. For the epoxy under investigation, tensile tests at various temperatures were run with the initial dry material. The results and the resulting linear relationship are shown in **Figure 11** with open-crossed squares and the solid line. As expected, the Eyring correlation is valid for the dry epoxy. In addition, the relation between T_g – T and tensile strength is also presented for the wet-aged epoxy. As before, a distinction is made between the aging temperature, environment, and duration. Compared with the prediction based on the dry specimens, it becomes clear that strong deviations are apparent for many wet-aged conditions. In detail, conditions can be identified that lead to both a significant underestimation and a significant overestimation of strength. On closer analysis, it becomes clear that the respective ranges can be assigned to specific physical conditions and equally form an upper and a lower limit. The lower limit is formed by the low temperature and above-T_g aged specimen; both have in common that their extent of additional physical aging is rather low. On the other hand, the upper limit is formed by the long-term and warm-condition aged specimen (40°C and 50°C) which should contain the highest proportion of physical aging and the strongest water–polymer interaction. All other temperature–duration combinations, however, fit within the complete range described by the two limits. Although some of these coincide well with the Eyring prediction, these matches are only valid for a given point in time. In any case, it is impossible to make a generally valid prediction of the strength based on the T_g, since the two properties develop dissimilarly as a function of temperature and duration.

3.8 Analysis of Water–Epoxy Interaction using DMTA

As already introduced in **Section 3.1**, DMTA can be used to analyze the thermo-mechanical response of polymers. For the case of hygrothermally aged polymers, the method is usually used

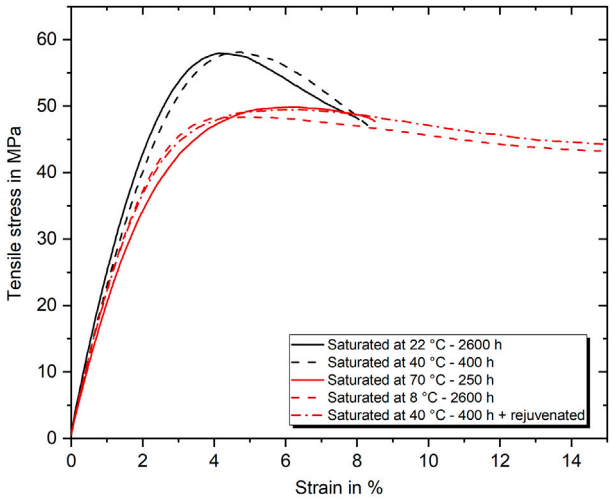

FIGURE 13 | Representative stress–strain curves of aging conditions resulting either in a strength of about 57 MPa (black) or 49 MPa (red).

to measure the T_g or its respective change during water absorption, as it is done within this study. Based on the broad hygrothermal aging conditions considered in this study, substantial differences in the expression of the tan(δ) behavior were additionally found. In **Figure 12** it is shown that the tan(δ) peak is split into two peaks. This is regularly observed and explained by the water diffusion (drying) during the test (Xian and Karbhari, 2007a,b). However, more surprising is the finding that the peak shape and, in detail, especially the width of the left base of the peak, show fundamental differences as a function of the aging temperature. While an inclination of the curve can be found even at temperatures as low as 35°C for aging at 8°C, the same inclination starts at above 60°C after aging in 50°C water. Assuming that there is always water saturation with only little deviations of water content in the samples at the beginning of the test, this result can be interpreted as a consequence of fundamentally different water-molecule–network interactions. Since tan(δ) is a measure of the energy that is, reversibly stored or dissipated, the earlier increase describes an earlier energy dissipation in the cold aged epoxy. In terms of the water-filled molecular network, this difference can result from water being mainly free or loosely bound (cold aging) or strongly bound (warm aging) to the network. In addition, it must be considered that accelerated physical aging may also be involved in these results. Considering the long-term aging results as well, it becomes clear that the typical curve shape of each aging type does not change substantially. With increased aging time, the curves of all conditions ≥22°C slightly shift to higher temperatures. In summary, the shape of the tan(δ) curve was found to be an indicator for the water-polymer network interaction, as it demonstrates significant differences. At the same time, the weight gain and T_g measurements and the FTIR peak evaluation don't show distinct deviations.

3.9 Comparison of Specific Time–Temperature Histories

The properties of specimens aged under particular conditions and tested subsequently at room temperature will be compared, as their mechanical properties or time-temperature aging history will allow drawing more detailed conclusions on the molecular interactions and processes acting during aging. The first pair of interest is the epoxy either aged at 40°C for 400 h or aged at 22°C for 2,600 h. After both aging procedures, the resulting strength is 57.0 MPa, the strain to failure is about 9.0%, and the water absorption amount is about 2.8 m%. Representative stress–strain curves are shown in **Figure 13** as black lines. As both conditions should theoretically be influenced by the same plasticizing effect of the absorbed water, equal yield strength and strain to failure could result from the same state of physical aging. However, in contrast, a first deviation can be found in Young's

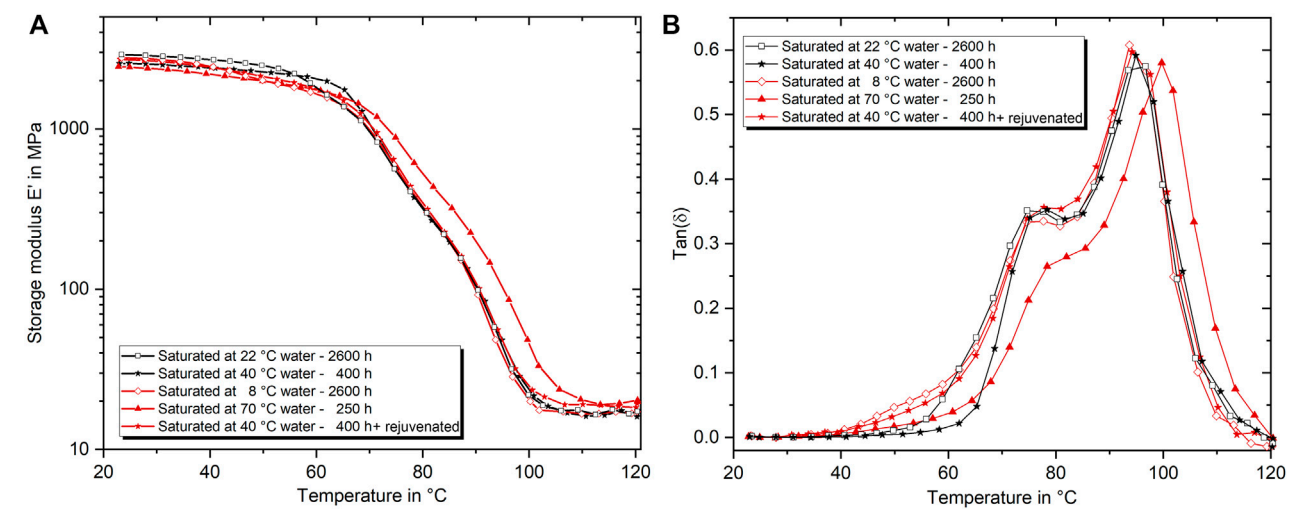

FIGURE 14 | Representative E′ **(A)** and tan(δ) **(B)** vs. temperature curves of aging conditions resulting either in a strength of about 57 MPa (black) or 49 MPa (red).

modulus evaluated from the tensile tests, which is about 0.2 GPa higher in the case of long-term room temperature aging. In addition, a comparison of the DMTA results of the same conditions also reveals significant differences. Especially the stiffness (in terms of the storage modulus E′), the T_g and the development of the loss factor tan(δ) differ clearly. While for the 40°C condition the storage modulus at 23°C is with 2.55 GPa considerable lower than 2.90 GPa for the 22°C condition, the T_g is with 64.7°C higher than 61.5°C. Furthermore, as shown with representative curves in **Figure 14**, the tan(δ) curves show clear differences in the peak width. In detail, the beginning of the tan(δ) increase is at particularly lower temperatures in case of the 22°C aging. Overall, it is evident from this comparison that even if the same amount of water is absorbed in the epoxy and the resulting strength and elongation at break are identical, the water-molecule interaction can differ significantly depending on the hygrothermal history.

The second set of remarkable conditions refers to the stages of low strength. The strength of long-term cold water (8°C) and short term hot water (70°C) saturated specimens, as well as specimens saturated at 40°C and subsequently rejuvenated, is all about 49 MPa. Nevertheless, distinct differences can be found in these cases as well. Noteworthy is especially the low stiffness of only 2.15 GPa but high T_g of 66.7°C after aging in 70°C water. As discussed in **Section 3.5**, the aging above wet T_g represents a unique case in which the physical aging should be suppressed to the most extent. As simultaneously the water content and the external activation energy by the environment are the highest, it can be hypothesized that the amount of strongly bound water is likewise very high. Furthermore, the drop in stiffness and increase in T_g show analogies to the development of these properties as a function of the curing degree identified by Antoniou et al. (2020) for a similar epoxy system. In this regard, the type II bound water could be expected to act like a secondary cross-linking, depressing the stiffness but increasing the T_g compared with sub-T_g aged conditions. However, the comparison of the Young's moduli of long term aged epoxy at 8°C (2.50 GPa) and 50°C (2.55 GPa), in contrast, reveals that the increased proportion of type II bound water slightly increases the stiffness, even though the absolute amount of absorbed water is higher after aging at 50°C. Therefore, the significant drop in stiffness after aging at 70°C is expected to be a result of the alongside running rejuvenation process due to aging above T_g and the high amount of absorbed water. Nevertheless, a shift of the tan(δ) peak base towards higher temperatures, thus, can be interpreted as a measure of type II bound water as it is shifted significantly for aging at high temperatures and long duration. It also fits that the strain to failure is significantly lower, since type II bound water should not contribute to plasticization. Following this argumentation, it also matches that both other configurations behave very similarly in all measured properties, as presented in **Figures 13**, **14**. While the increase in physical aging should be minimal with aging at 8°C, the rejuvenation process resets the physical aging after saturation at 40°C as well. The small differences in stiffness (0.2 GPa) and tan(δ) behavior, again, follow the proposed argumentation and might be mainly explained by the increased free volume and higher amount of absorbed water in the case of the 40°C rejuvenated specimens. For the rejuvenated case, it is suspected that the process temperature is not high enough to dissolve the type II bindings, which have formed during aging. This is in line with the findings of Zhou and Lucas (1999a) proposing the need of very high temperatures to remove type II bound water.

4 CONCLUSION

In summary, the results presented show a strong dependence of the mechanical properties on the time-temperature history of hygrothermal aging. Considering water absorption and thermo-mechanical analyses, it can be assumed that not all properties will converge to the same values for different operating temperatures, even after extremely long periods. The main reason for this is considered to be the different amount of free water acting as a plasticizer and strongly bound water acting as additional crosslinking. The main outcomes are concluded as follows:

- The maximum amount of water that the epoxy can absorb is temperature-dependent up to an ambient temperature of 50°C. This is most likely due to the lower number of attractive molecular segments that can be reached since the mobility is strongly limited at low temperatures.
- The tensile strength of the epoxy is not only a function of the absorbed water content but rather a function of the aging history, which includes time and temperature. For the investigated epoxy, the tensile strength after long-term aging was found to be between 48 MPa after cold water aging and 65 MPa after warm water aging, which is a difference of 26.1%. Over time, the strength increases due to relaxation, whereas the speed of this process is strongly temperature-dependent. Since the amount of water absorption and the form in which the water is present in the epoxy can be quite different depending on the temperature, it is assumed that even after an extremely long aging duration, differences will be present.
- As the strength and the T_g show basically different behaviors over time and aging temperature, T_g-based strength predictions as typically used with the Eyring correlations are not sufficient. Instead, it was revealed that the strength–T_g relationship is strongly dependent on the state of physical aging. An upper and lower limit with strength differences of up to 16 MPa or 30%, respectively, could be described for the same distance between T_g and testing temperature. This is mainly because the T_g decreases dramatically due to the plasticizing effect of water but increases only marginally due to physical aging or strongly bound water (type II).
- Long-term aging of up to 2,600 h at elevated temperatures demonstrated that the epoxy can regain up to about 93% of its dry strength, even though the polymer is saturated with about 3% of water. However, the high strength is then accompanied by a slightly reduced fracture strain.
- With the help of thermo-mechanical investigations and thermally rejuvenated specimens, differences in the degree of physical aging and in the amount of strongly bound water could be identified. For identical T_g, weight gain, and strength, the peak shape of tan(δ) allows revealing significant differences between aging conditions.
- As disclosed by aging in various ambient temperatures below and above the epoxy's wet-T_g, the amount of strongly bound

water (type II) is expected to increase significantly with higher temperatures. When considering T_g development over time, it can also be assumed that almost no type II bonds are formed at temperatures of less than 40°C. For lower temperatures, the T_g, therefore, also shows a time-independent linear behavior with the water content, which can be modeled using the well-known Simha-Boyer equation or other polymer-diluent models. For higher temperatures, the T_g increases over time.

- For the application of accelerated aging methods, it was shown that the hygro-mechanical properties of the epoxy are already strongly influenced by relatively low aging temperatures. In particular, especially the substantial strength decrease at cold conditions or the pronounced physical aging process could be easily overseen or misinterpreted by accelerated aging only.

DATA AVAILABILITY STATEMENT

The raw data supporting the conclusion of this article will be made available by the authors, without undue reservation.

AUTHOR CONTRIBUTIONS

All authors listed have made a substantial, direct, and intellectual contribution to the work and approved it for publication. DG: Conceptualization, Methodology, Investigation, Writing—Original Draft, Visualization; CB: Methodology, Writing—Review Editing DM: Methodology, Investigation; BF: Conceptualization, Writing—Review and Editing, Supervision.

FUNDING

We acknowledge support for the Open Access fees by Hamburg University of Technology (TUHH) in the funding program Open Access Publishing.

ACKNOWLEDGMENTS

The authors would like to thank Hexion for providing the epoxy system.

REFERENCES

Abdelkader, A. F., and White, J. R. (2005). Water Absorption in Epoxy Resins: The Effects of the Crosslinking Agent and Curing Temperature. *J. Appl. Polym. Sci.* 98, 2544–2549. doi:10.1002/app.22400

Amano, R. S. (2017). Review of Wind Turbine Research in 21st century. *J. Energ. Resour. Technol.* 139, 051201. doi:10.1115/1.4037757

Antoniou, A., Rosemeier, M., Tazefidan, K., Krimmer, A., and Wolken-Möhlmann, G. (2020). Impact of Site-specific thermal Residual Stress on the Fatigue of Wind-Turbine Blades. *AIAA J.* 58, 4781–4793. doi:10.2514/1.J059388

Banea, M. D., de Sousa, F. S. M., da Silva, L. F. M., Campilho, R. D. S. G., and de Pereira, A. M. B. (2011). Effects of Temperature and Loading Rate on the Mechanical Properties of a High Temperature Epoxy Adhesive. *J. Adhes. Sci. Technol.* 25, 2461–2474. doi:10.1163/016942411X580144

Bellenger, V., Verdu, J., and Morel, E. (1989). Structure-properties Relationships for Densely Cross-Linked Epoxide-Amine Systems Based on Epoxide or Amine Mixtures. *J. Mater. Sci.* 24, 63–68. doi:10.1007/BF00660933

Bordes, M., Davies, P., Cognard, J.-Y., Sohier, L., Sauvant-Moynot, V., and Galy, J. (2009). Prediction of Long Term Strength of Adhesively Bonded Steel/epoxy Joints in Sea Water. *Int. J. Adhes. Adhesives* 29, 595–608. doi:10.1016/j.ijadhadh.2009.02.013

Budhe, S., Banea, M. D., and de Barros, S. (2018). Bonded Repair of Composite Structures in Aerospace Application: a Review on Environmental Issues. *Appl. Adhes. Sci.* 6, 1797. doi:10.1186/s40563-018-0104-5

Capiel, G., Uicich, J., Fasce, D., and Montemartini, P. E. (2018). Diffusion and Hydrolysis Effects during Water Aging on an Epoxy-Anhydride System. *Polym. Degrad. Stab.* 153, 165–171. doi:10.1016/j.polymdegradstab.2018.04.030

Chai, H. (2004). The Effects of Bond Thickness, Rate and Temperature on the Deformation and Fracture of Structural Adhesives under Shear Loading. *Int. J. Fracture* 130, 497–515. doi:10.1023/B:FRAC.0000049504.51847

Colin, X. (2018). "Nonempirical Kinetic Modeling of Non-fickian Water Absorption Induced by a Chemical Reaction in Epoxy-Amine Networks," in *Durability of Composites in a Marine Environment 2. Of Solid Mechanics and its Applications*. Editors P. Davies and Y. D. Rajapakse (Cham: Springer International Publishing, Vol. 245. doi:10.1007/978-3-319-65145-3\\text{_}110.1007/978-3-319-65145-3_1

Cotugno, S., Larobina, D., Mensitieri, G., Musto, P., and Ragosta, G. (2001). A Novel Spectroscopic Approach to Investigate Transport Processes in Polymers: the Case of Water-Epoxy System. *Polymer* 42, 6431–6438. doi:10.1016/S0032-3861(01)00096-9

Ding, Y., Liu, M., Li, S., Zhang, S., Zhou, W.-F., and Wang, B. (2001). Contributions of the Side Groups to the Characteristics of Water Absorption in Cured Epoxy Resins. *Macromol. Chem. Phys.* 202, 2681–2685. doi:10.1002/1521-393510.1002/1521-3935(20010901)202:13<2681:aid-macp2681>3.0.co;2-e

Doblies, A., Feiler, C., Würger, T., Schill, E., Meißner, R. H., and Fiedler, B. (2021). Mechanical Degradation Estimation of Thermosets by Peak Shift Assessment: General Approach Using Infrared Spectroscopy. *Polymer* 221, 123585. doi:10.1016/j.polymer.2021.123585

Elkebir, Y., Mallarino, S., Trinh, D., and Touzain, S. (2020). Effect of Physical Ageing onto the Water Uptake in Epoxy Coatings. *Electrochimica Acta* 337, 135766. doi:10.1016/j.electacta.2020.135766

Enns, J. B., and Gillham, J. K. (1983). Effect of the Extent of Cure on the Modulus, Glass Transition, Water Absorptio, and Density of an Amine-Cured Epoxy. *J. Appl. Polym. Sci.* 28, 2831–2846. doi:10.1002/app.1983.070280914

Fernández-García, M., and Chiang, M. Y. M. (2002). Effect of Hygrothermal Aging History on Sorption Process, Swelling, and Glass Transition Temperature in a Particle-Filled Epoxy-Based Adhesive. *J. Appl. Polym. Sci.* 84, 1581–1591. doi:10.1002/app.10447

Gagani, A. I., Monsås, A. B., Krauklis, A. E., and Echtermeyer, A. T. (2019). The Effect of Temperature and Water Immersion on the Interlaminar Shear Fatigue of Glass Fiber Epoxy Composites Using the I-Beam Method. *Composites Sci. Technol.* 181, 107703. doi:10.1016/j.compscitech.2019.107703

Gaudichet-Maurin, E., Thominette, F., and Verdu, J. (2008). Water Sorption Characteristics in Moderately Hydrophilic Polymers, Part 1: Effect of Polar Groups Concentration and Temperature in Water Sorption in Aromatic Polysulfones. *J. Appl. Polym. Sci.* 109, 3279–3285. doi:10.1002/app.24873

Humeau, C., Davies, P., and Jacquemin, F. (2018). An Experimental Study of Water Diffusion in Carbon/epoxy Composites under Static Tensile Stress. *Composites A: Appl. Sci. Manufacturing* 107, 94–104. doi:10.1016/j.compositesa.2017.12.016

Ilioni, A., Le Gac, P.-Y., Badulescu, C., Thévenet, D., and Davies, P. (2019). Prediction of Mechanical Behaviour of a Bulk Epoxy Adhesive in a marine Environment. *J. Adhes.* 95, 64–84. doi:10.1080/00218464.2017.1377616

Jaksic, V., Kennedy, C. R., Grogan, D. M., Leen, S. B., and Brádaigh, C. M. Ó. (2018). "Influence of Composite Fatigue Properties on marine Tidal Turbine Blade Design,".*Durability of Composites in a Marine Environment 2 of Solid Mechanics and its Applications.* Editors P. Davies and Y. D. Rajapakse (Cham: Springer International Publishing,. doi:10.1007/978-3-319-65145-3\\text{_}1110.1007/978-3-319-65145-3_11

Kambour, R. P. (1983). Correlations of the Dry Crazing Resistance of Glassy Polymers with Other Physical Properties. *Polym. Commun.*

Krauklis, A. E., Gagani, A. I., and Echtermeyer, A. T. (2018a). Hygrothermal Aging of Amine Epoxy: Reversible Static and Fatigue Properties. *Open Eng.* 8, 447–454. doi:10.1515/eng-2018-0050

Krauklis, A., Gagani, A., and Echtermeyer, A. (2018b). Near-infrared Spectroscopic Method for Monitoring Water Content in Epoxy Resins and Fiber-Reinforced Composites. *Materials* 11, 586. doi:10.3390/ma11040586

Kraus, D., and Trappe, V. (2021). Transverse Damage in Glass Fiber Reinforced Polymer under Thermo-Mechanical Loading. *Composites C: Open Access* 5, 100147. doi:10.1016/j.jcomc.2021.100147

LaPlante, G., Ouriadov, A. V., Lee-Sullivan, P., and Balcom, B. J. (2008). Anomalous Moisture Diffusion in an Epoxy Adhesive Detected by Magnetic Resonance Imaging. *J. Appl. Polym. Sci.* 109, 1350–1359. doi:10.1002/app.28106

Le Gac, P.-Y., Arhant, M., Le Gall, M., and Davies, P. (2017). Yield Stress Changes Induced by Water in Polyamide 6: Characterization and Modeling. *Polym. Degrad. Stab.* 137, 272–280. doi:10.1016/j.polymdegradstab.2017.02.003

Le Guen-Geffroy, A., Le Gac, P.-Y., Habert, B., and Davies, P. (2019). Physical Ageing of Epoxy in a Wet Environment: Coupling between Plasticization and Physical Ageing. *Polym. Degrad. Stab.* 168, 108947. doi:10.1016/j.polymdegradstab.2019.108947

Muroga, S., Hikima, Y., and Ohshima, M. (2017). Near-infrared Spectroscopic Evaluation of the Water Content of Molded Polylactide under the Effect of Crystallization. *Appl. Spectrosc.* 71, 1300–1309. doi:10.1177/0003702816681011

Musto, P., Ragosta, G., and Mascia, L. (2000). Vibrational Spectroscopy Evidence for the Dual Nature of Water Sorbed into Epoxy Resins. *Chem. Mater.* 12, 1331–1341. doi:10.1021/cm9906809

Musto, P., Ragosta, G., Scarinzi, G., and Mascia, L. (2002). Probing the Molecular Interactions in the Diffusion of Water through Epoxy and Epoxy-Bismaleimide Networks. *J. Polym. Sci. B Polym. Phys.* 40, 922–938. doi:10.1002/polb.10147

Papanicolaou, G. C., Kosmidou, T. V., Vatalis, A. S., and Delides, C. G. (2006). Water Absorption Mechanism and Some Anomalous Effects on the Mechanical and Viscoelastic Behavior of an Epoxy System. *J. Appl. Polym. Sci.* 99, 1328–1339. doi:10.1002/app.22095

Rocha, I. B. C. M., Raijmaekers, S., van der Meer, F. P., Nijssen, R. P. L., Fischer, H. R., and Sluys, L. J. (2017). Combined Experimental/numerical Investigation of Directional Moisture Diffusion in Glass/epoxy Composites. *Composites Sci. Technol.* 151, 16–24. doi:10.1016/j.compscitech.2017.08.002

Startsev, V. O., Lebedev, M. P., Khrulev, K. A., Molokov, M. V., Frolov, A. S., and Nizina, T. A. (2018). Effect of Outdoor Exposure on the Moisture Diffusion and Mechanical Properties of Epoxy Polymers. *Polym. Test.* 65, 281–296. doi:10.1016/j.polymertesting.2017.12.007

Tcharkhtchi, A., Nony, F., Khelladi, S., Fitoussi, J., and Farzaneh, S. (2015). "Epoxy/amine Reactive Systems for Composites Materials and Their Thermomechanical Properties," in *Advances in Composites Manufacturing and Process Design* (Elsevier), 43, 269–296. doi:10.1016/B978-1-78242-307-2.00013-0

Tcharkhtchi, A., Trotignon, J.-P., and Verdu, J. (1999). Yielding and Fracture in Crosslinked Epoxies. *Macromol. Symp.* 147, 221–234. doi:10.1002/masy.19991470122

Xian, G., and Karbhari, V. M. (2007a). Dmta Based Investigation of Hygrothermal Ageing of an Epoxy System Used in Rehabilitation. *J. Appl. Polym. Sci.* 104, 1084–1094. doi:10.1002/app.25576

Xian, G., and Karbhari, V. M. (2007b). Segmental Relaxation of Water-Aged Ambient Cured Epoxy. *Polym. Degrad. Stab.* 92, 1650–1659. doi:10.1016/j.polymdegradstab.2007.06.015

Zheng, Y., Priestley, R. D., and McKenna, G. B. (2004). Physical Aging of an Epoxy Subsequent to Relative Humidity Jumps through the Glass Concentration. *J. Polym. Sci. B Polym. Phys.* 42, 2107–2121. doi:10.1002/polb.20084

Zhou, J., and Lucas, J. P. (1999a). Hygrothermal Effects of Epoxy Resin. Part I: the Nature of Water in Epoxy. *Polymer* 40, 5505–5512. doi:10.1016/S0032-3861(98)00790-3

Zhou, J., and Lucas, J. P. (1999b). Hygrothermal Effects of Epoxy Resin. Part Ii: Variations of Glass Transition Temperature. *Polymer* 40, 5513–5522. doi:10.1016/S0032-3861(98)00791-5

Conflict of Interest: The authors declare that the research was conducted in the absence of any commercial or financial relationships that could be construed as a potential conflict of interest.

Publisher's Note: All claims expressed in this article are solely those of the authors and do not necessarily represent those of their affiliated organizations, or those of the publisher, the editors, and the reviewers. Any product that may be evaluated in this article, or claim that may be made by its manufacturer, is not guaranteed or endorsed by the publisher.

Copyright © 2022 Gibhardt, Buggisch, Meyer and Fiedler. This is an open-access article distributed under the terms of the Creative Commons Attribution License (CC BY). The use, distribution or reproduction in other forums is permitted, provided the original author(s) and the copyright owner(s) are credited and that the original publication in this journal is cited, in accordance with accepted academic practice. No use, distribution or reproduction is permitted which does not comply with these terms.